Concurrent Dual-Band Shifter With Independent Tunable Phase Shift Control

Samdy Saron, *Student Member, IEEE*, Girdhari Chaudhary, *Member, IEEE*, and Yongchae Jeong, *Senior Member, IEEE*

***Abstract*— This article presents a design of a reflection-type dual-band phase shifter (DPS) that allows to tuning relative phase shifts at two operating frequency bands independently. The proposed phase shifter consists of a 3-dB hybrid coupler where through and a couple of ports are terminated with reflection loads. Each reflection load comprises a couple of lines terminated with a transmission line (TL) and a varactor diode. The coupled line can achieve independent phase tuning at each operating frequency, while TL terminated with a varactor diode is used for a high relative phase shift tuning range (PSR). The proposed tunable DPS can provide not only independent tunable phase shift (ITPS) at each operating band, but also simultaneous tunable phase shift at both bands. To prove the validity of the proposed method, the DPS operating at center frequencies of 1.88 and 2.44 GHz is designed and fabricated. The measured relative PSR is 149.33° at 1.88 GHz with phase derivation error (PDE) of ±8.45° within 300 MHz bandwidth (BW). Similarly, the PSR at 2.44 GHz is 125.25° with a PDE of ±8.36° within the same BW of 300 MHz. Likewise, the minimum return loss (RL) of around 17.36 dB, and the maximum insertion loss (IL) of 1.81 dB are measured at both operating bands.**

***Index Terms*— Concurrent dual-band tunable phase shifter, coupled line, independent phase control, varactor diode.**

I. Introduction

A TUNABLE phase shifter is used to control a phase of a signal which has been found wide range of various applications including beamforming [1], phased array antenna [2], and self-interference cancellation [3]. To support multiband wireless communications, it is necessary to design a tunable phase shifter that operates over multiple frequency bands simultaneously. However, previously reported tunable phase shifters are mainly designed for single-frequency band operations, which fail to provide independently controllable transmission phase shift over multiband frequency operation [4], [5], [6], [7].

Recently, a dual-band 90° SiGe HBT active phase shifter is presented in [8] using bandpass and bandstop filters in the load circuit. In [9], a dual-band phase shifter (DPS) is designed by using two stub-loaded transmission lines (TLs) and two delay lines. Similarly, a dual-band differential phase shifter is presented in [10] that utilized slope alignment of coupled line resonators.

Manuscript received 3 August 2023; revised 1 December 2023; accepted 19 December 2023. Date of publication 3 January 2024; date of current version 13 February 2024. This work was supported in part by the National Research Foundation of Korea (NRF) grant funded by the Korean Government (MSIT) under Grant RS-2023-00209081 and in part by the Basic Science Research Program through the NRF grant funded by the Ministry of Education under Grant 2019R1A6A1A09031717. *(Corresponding author: Yongchae Jeong.)*

The authors are with the Division of Electronic and Information Engineering, Jeonbuk National University, Jeonju-si 54896, Republic of Korea (e-mail: girdharic@jbnu.ac.kr; ycjeong@jbnu.ac.kr).

Color versions of one or more figures in this letter are available at https://doi.org/10.1109/LMWT.2023.3345950.

Digital Object Identifier 10.1109/LMWT.2023.3345950

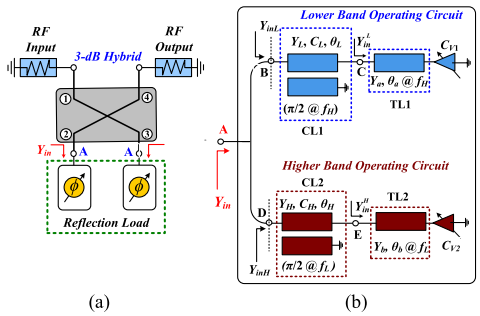

(a) (b)

Fig. 1. (a) Proposed structure of a reflection-type dual-band tunable phase shifter and (b) circuit implementation of tunable reflection load.

However, these DPSs cannot provide independent tunable phase shifts (ITPS) at two operating bands. A concurrent dual-band monolithic microwave integrated circuit (MMIC) tunable phase shifter is reported in [11] utilizing a two-stage dual-branch phase tuning network topology. A reflection-type DPS with ITPS is presented in [12] using $\lambda/4$ series and shunt TLs. However, this work requires compensation shunt elements at each operating band to compensate for the parasitic effect of $\lambda/4$ shunt TL for achieving ITPS and a high relative phase shift tuning range (PSR).

In this article, a reflection-type dual-band tunable phase shifter is proposed using coupled lines terminated with TLs and varactor diodes, which do not require any compensation elements. The coupled lines have been utilized for achieving independent phase control at each operating band as well as improving PSR. The proposed DPS can provide an independent tunable phase at each operating band as well as a simultaneous tunable phase shift at both bands.

II. Design Theory

Fig. 1(a) depicts the proposed structure of a reflection-type tunable DPS that consists of a 3-dB hybrid where through and coupled ports are terminated with reflection loads. Fig. 1(b) shows the reflection load that consists of coupled lines terminated TL and varactor diode operating at lower and higher band frequencies. The tunable phase operation at a high or low band can affect other low or high bands, and these interferences must be prevented to achieve an independent phase shift at each operating band. Therefore, it is necessary to cancel the interference effect so that the proposed DPS can provide an independent tunable phase at each operating band as well as a simultaneous tunable phase shift at both bands.

To achieve independent phase control at each band, the coupled lines are used. The total input admittance looking at point A in Fig. 1(b) is given as (1), where f, f_L, and f_H are operating frequency, lower band center frequency, and higher band center frequency, respectively,

$$Y_{in} = Y_{inL} + Y_{inH} \tag{1}$$

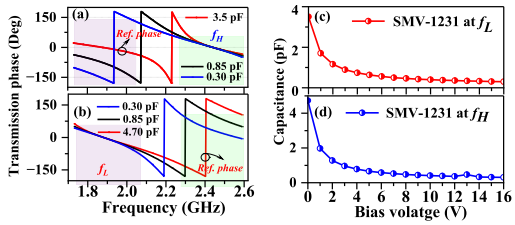

Fig. 2. Phase variation in cases. (a) C_{V1} is varied from 0.3 to 3.5 pF, while C_{V2} is fixed at 4.7 pF. (b) C_{V2} is varied from 0.3 to 3.5 pF, while C_{V1} is fixed at 3.5 pF. Other circuit parameters: $Z_L = 1/Y_L = 81\ \Omega$, $C_L = -8.3$ dB, $Z_a = 1/Y_a = 120\ \Omega$, $\theta_a = 110°$, $Z_H = 1/Y_H = 70\ \Omega$, $C_H = -7$ dB, $Z_b = 1/Y_b = 120\ \Omega$, and $\theta_b = 123°$. Capacitance variation according to bias voltage at (c) f_L and (d) f_H.

TABLE I

CALCULATED PSR $= \Delta\varphi_{MAX}$ AND PDE $= \varphi_{ERR}$ WITHIN BW OF 300 MHZ AT $f_L = 1.88$ GHZ FOR DIFFERENT CIRCUIT PARAMETERS

Varactor diode SMV-1231 with C_V: 0.3 pF to 3.5 pF					
$Z_L\,(\Omega)$	C_L (dB)	$Z_a\,(\Omega)$	$\theta_a\,(°)$	$\Delta\varphi_{max}\,(°)$	$\varphi_{err}\,(°)$
70	-8	120	117	142.16	±9.76
70	-8.5		123	134.83	±8.97
80	-8		110	151.34	±8.84
81	-8.3		110	146.15	±6.72
85	-8.5		117	143.65	±9.89

where

$$Y_{inL,H} = j\frac{\left[\left(Y_{11}^{L,H}\right)^2 - \left(Y_{12}^{L,H}\right)^2\right]\left[\left(Y_{in}^{L,H}\right)^2 + \left(Y_{11}^{L,H}\right)^2\right] - A - B + C}{D} \tag{2a}$$

$$A = j^4\left[\left(Y_{14}^{L,H}\right)^2 + \left(Y_{24}^{L,H}\right)^2\right]\left[\left(Y_{11}^{L,H}\right)^2 + Y_{11}^{L,H}Y_{in}^{L,H}\right] \tag{2b}$$

$$B = 2j^4 Y_{in}^{L,H}Y_{12}^{L,H}\left(Y_{12}^{L,H}Y_{44}^{L,H} - Y_{42}^{L,H}Y_{14}^{L,H}\right) \tag{2c}$$

$$C = 2j^4\left[\left(Y_{11}^{L,H}\right)^3 Y_{in}^{L,H} + Y_{44}^{L,H}Y_{12}^{L,H}Y_{42}^{L,H}Y_{14}^{L,H}\right] \tag{2d}$$

$$D = j^3\left[\begin{array}{l}\left(Y_{in}^{L,H}\right)^2 Y_{22}^{L,H} + \left(Y_{44}^{L,H}\right)^2\left(2Y_{in}^{L,H} + Y_{44}^{L,H}\right) \\ -\left(Y_{24}^{L,H}\right)^2\left(Y_{in}^{L,H} + Y_{44}^{L,H}\right)\end{array}\right] \tag{2e}$$

$$Y_{11}^{L,H} = -j\frac{Y_{L,H}}{\sqrt{1-K_{L,H}^2}}\cot\theta_{L,H},\quad Y_{12}^{L,H} = -j\frac{K_{L,H}Y_{L,H}}{\sqrt{1-K_{L,H}^2}} \times \cot\theta_{L,H} \tag{2f}$$

$$Y_{42}^{L,H} = -j\frac{K_{L,H}Y_{L,H}}{\sqrt{1-K_{L,H}^2}}\csc\theta_{L,H},\quad Y_{14}^{L,H} = -j\frac{Y_{L,H}}{\sqrt{1-K_{L,H}^2}} \times \csc\theta_{L,H} \tag{2g}$$

$$\theta_L = \frac{\pi f}{2f_H},\quad \theta_H = \frac{\pi f}{2f_L} \tag{2h}$$

$$Y_{in}^{L} = -j\frac{2\pi f Y_a C_{V1} + Y_a^2\tan\frac{\theta_a f}{f_H}}{Y_a - 2\pi f C_{V1}\tan\frac{\theta_a f}{f_H}}$$

$$Y_{in}^{H} = -j\frac{2\pi f Y_b C_{V2} + Y_b^2\tan\frac{\theta_b f}{f_L}}{Y_b - 2\pi f C_{V2}\tan\frac{\theta_b f}{f_L}} \tag{2i}$$

$$K_L = 10^{[-C_L(dB)/20]},\quad K_H = 10^{[-C_H(dB)/20]} \tag{2j}$$

$Y_{a,b}$, $\theta_{a,b}$, and C_V are characteristic admittances, electrical lengths of the TL, and capacitance of the varactor diode, respectively. Likewise, $Y_{L,H} = 1/Z_{L,H}$ and $K_{L,H}$ are characteristic admittances and coupling coefficients of coupled line, which are expressed in terms of even and odd-mode admittances as depicted in the following equation:

$$Y_{0eL,H} = Y_{L,H}\sqrt{\frac{1+K_{L,H}}{1-K_{L,H}}},\quad Y_{0oL,H} = Y_{L,H}\sqrt{\frac{1-K_{L,H}}{1+K_{L,H}}}. \tag{3}$$

Using (1) and (2), the phase of the proposed DPS can be written as follows:

$$\varphi = \pi - 2\tan^{-1}\left(\frac{Y_{inL} + Y_{inH}}{Y_0}\right) \tag{4}$$

where $Y_0 = 1/Z_0$ is a port termination admittance. From (1)–(4), it should be noted that the coupled line (CL1) provides an open condition ($Y_{inL} = 0$) when $f = f_H$, while CL1 acts as a capacitance at f_L. As a result, no phase shift occurs at f_H while tuning phase shift occurs at f_L. Likewise, the coupled line provides an open condition ($Y_{inH} = 0$) when $f = f_L$, while CL2 acts as an inductance at f_H, then no phase shift changes at f_L, and the phase shift is controlled at f_H. Therefore, the proposed tunable DPS provides independent controllable phase shifts at two operating bands.

Fig. 2(a) and (b) shows ITPS characteristics at lower and higher operating bands. As seen in the figure, the transmission phase shift is independently tuned at a lower operating frequency band (1.73∼2.03 GHz) when C_{V1} is varied and C_{V2} is fixed as shown in Fig. 2(a). Fig. 2(b) depicts that the phase shift is also independently controlled at a higher operating frequency band (2.29∼2.59 GHz) while tuning C_{V2} and fixing C_{V1}. This independent phase shift control is achieved due to coupled lines.

To achieve high relative PSR with low phase derivation error (PDE) within a certain operating frequency bandwidth (BW), proper circuit parameter selections of coupled lines and TLs are necessary. For this purpose, the capacitance of varactor diode SMV1231 from Skyworks Inc is measured, which provides capacitance variation of 0.3–3.5 pF at f_L, as shown in Fig. 2(c) and 0.3–4.7 pF at f_H when dc-bias voltage is varied from 16 to 0 V is illustrated in Fig. 2 (d). The circuit parameters of coupled lines and TLs are optimized for each operating center frequency by using MATLAB and results are shown in Tables I and II. As seen from Table I, the maximum relative PSR of 146° is achieved at lower operating center frequency $f_L = 1.88$ GHz with PDE of ±6.72° within BW of 300 MHz, when circuit parameters are selected as $Z_L = 1/Y_L = 81\ \Omega$, $C_L = -8.3$ dB, $Z_a = 1/Y_a = 120\ \Omega$, and $\theta_a = 110°$. Similarly, the maximum relative PSR of 130.6° is achieved at f_H with PDE of ±8.64° within BW of 300 MHz,

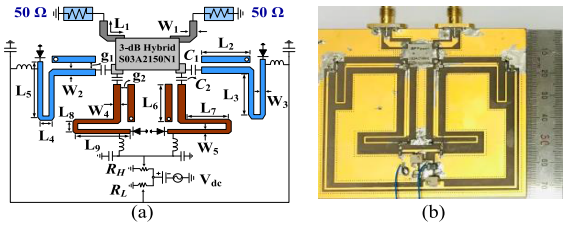

Fig. 3. (a) Microstrip line implementation of the proposed fully dual-band tunable phase shifter. Physical dimensions: $W_1 = 2.35$, $L_1 = 12.8$, $W_2 = 0.8$, $L_2 = 22.6$, $g_1 = 0.15$, $W_3 = 0.5$, $L_3 = 15.75$, $L_4 = 3$, $L_5 = 17.55$, $W_4 = 0.9$, $L_6 = 30.7$, $W_5 = 0.5$, $L_7 = 15.75$, $g_2 = 0.15$, $L_8 = 2$, and $L_9 = 17.55$. Unit: millimeter (mm). dc block: $C_1 = 56.6$ pF, $C_2 = 120$ pF. Varactor SMV 1231 from Skyworks Inc. Variable resistors: $R_{L,H} = 10$ kΩ SMD potentiometer from Bourns Inc. (b) Photograph of fabricated DPS.

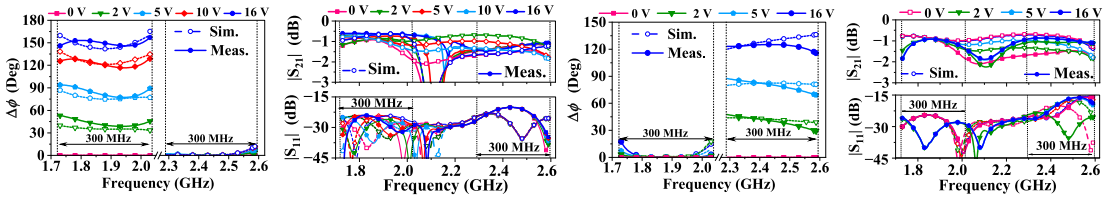

Fig. 4. Simulation and measurement results. (a) PSR of the first case. (b) *S*-parameter response of the first case. (c) PSR of the second case. (d) *S*-parameter response of the second case.

TABLE II

CALCULATED PSR = $\Delta\varphi_{MAX}$ AND PDE = φ WITHIN BW OF 300 MHZ AT f_L = 2.44 GHZ FOR DIFFERENT CIRCUIT PARAMETERS

Varactor diode SMV-1231 with C_T: 0.3 pF to 4.7 pF					
Z_H (Ω)	C_H(dB)	Z_b (Ω)	θ_b (°)	$\Delta\varphi_{max}$ (°)	φ_{err} (°)
61	-7	110	128	135.5	±8.82
65	-7	120	125	127.14	±8.48
70	-7		123	130.6	±8.64
71	-6.9		123	133.23	±9.36
72	-7.1		123	130.62	±9.48

when circuit parameters are selected as $Z_H = 1/Y_H = 70\ \Omega$, $C_H = -7$ dB, $Z_b = 1/Y_b = 120\ \Omega$, and $\theta_b = 123°$.

III. EXPERIMENTAL RESULTS

For experimental validation, a prototype of tunable DPS operating at $f_L = 1.88$ GHz and $f_H = 2.44$ GHz is designed and fabricated using a Taconic substrate with a dielectric constant of 2.2 and thickness of 0.787 mm. Fig. 3(a) depicts the physical layout of the fabricated circuit with dimensions. The photograph of the fabricated circuit is shown in Fig. 3(b) its size is $0.9\lambda_g \times 0.8\lambda_g$. In this work, a 3-dB hybrid coupler S03A2500N1 from ANAREN is used.

Figs. 4 and 5 show simulation and measurement results. The measurement results agreed with the simulations. The performances of the proposed phase shifter are investigated in three cases. In the first case, the bias voltage of the varactor diode operating at lower band f_L is varied from 0 to 16 V, while the bias voltage of the varactor diode operating at higher band f_H is fixed at 0 V. In this case, the measured maximum PSR of 149.32° with PDE of ±8.25° is achieved within BW of 300 MHz at f_L, while maintaining 0° phase shift at f_H, as shown in Fig. 4(a). Furthermore, insertion loss (IL) smaller than 1.96 dB and input–output return losses larger than 20.16 dB are measured at both operating bands.

In the second case, the bias voltage of the varactor diode operating at f_L is fixed to 0 V, while the bias voltage of the varactor diode operating at f_H is varied from 0 to 16 V. The simulation and measured results of the second case are shown in Fig. 4(b). From the measurement, a maximum PSR of 125.14° and PDE of ±9.34° are obtained within 300 MHz BW of f_H. Moreover, IL smaller than 1.84 dB and input–output return losses larger than 16.14 dB are measured at both operating bands.

Fig. 5 shows the simulation and measurement results of the third case where relative phase shifts at both operating bands are tuned simultaneously. In this case, the maximum PSR of 149.33° with PDE of ±8.45° is measured within BW of 300 MHz at f_L, while the maximum PSR of 125.25° with PDE of ±8.36° is measured within BW of 300 MHz at f_H. The measured insertion losses vary from 1 to 1.84 dB at f_L and from 1.1 to 1.81 dB at f_H. The IL can be improved by using a varactor diode with low parasitic resistance. While tuning relative PSR, the measured input–output return losses

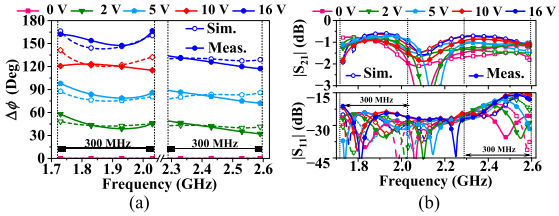

Fig. 5. Simulation and measurement results of the third case. (a) PSR and (b) *S*-parameter responses.

TABLE III

PERFORMANCE COMPARISON WITH STATE-OF-THE-ARTS

	f_0 (GHz)	BW (GHz)	FBW (%)	PSR (°)	PDE (°)	IL (dB)	RL_{min} (dB)	D/I	FOM
[10]	1.46 4.35	0.47 0.45	32.2 10.34	90* 270*	±5 ±5	<0.73 <1.28	>15 >15	Y/N	NA
[11]	5.9 16	0.2 0.4	3.39 2.5	106 108	±7 ±7	<2.8 <3.5	>10 >10	Y/Y	1.18 0.82
[12]	1.88 2.44	0.1 0.1	5.32 4	114 114	±8.4 ±5.4	<1.86 <1.89	>19.7 >16.8	Y/Y	5.60 4.83
This Work	**1.88** **2.44**	**0.3** **0.3**	**15.96** **12.30**	**149.33** **125.25**	**±8.45** **±8.36**	**<1.84** **<1.81**	**>21.1** **>17.3**	**Y/Y**	**26.08** **10.96**

FBW: Fractional Bandwidth, PSR: Relative phase shift range, PDE: phase derivation error within certain bandwidth. D: Dual-band phase shifter, I: independent control phase shift, *: differential phase shifter with fixed phase shift.

are higher than 21.1 dB at a lower band operating frequency and 17.36 dB at a higher band operating frequency.

Table III shows the performance comparison of the proposed tunable DPS with previously reported works. In this work, the figure of merit (FoM) is defined as (5) by considering PSR, IL, return loss (RL), and BW

$$\text{FoM} = \frac{\text{BW(GHz)} \times \text{PSR(rad)}}{f_0\text{(GHz)} \times \text{PDE(rad)}} \times \frac{10^{\left(\frac{-\text{IL}(dB)}{20}\right)}}{10^{\left(\frac{-\text{RL}(dB)}{20}\right)}}. \quad (5)$$

Most of the previously reported tunable phase shifters are designed for single-band frequency operation [4], [5], [6], [7]. In comparison to previously reported DPSs, the proposed work provides high PSR with the highest FoM. Furthermore, the proposed dual-band tunable phase shifter allows independent phase shift tuning at each operating frequency as well as simultaneous phase shift tuning at both bands.

IV. CONCLUSION

This article presented a design of reflection-type tunable DPS that allows to control independent phase shift at each operating band as well as simultaneous tunable phase shift at both bands. For experimental validation, a prototype of tunable DPS is designed and fabricated at operating center frequencies of 1.88 and 2.44 GHz. The proposed dual-band provides a high relative phase shift range with flat phase characteristics within 300 MHz BW. The ability of independent phase shift control in different operating frequency bands makes the proposed dual-band tunable phase shifter valuable in wireless communication systems, radar, and phased array antennas that require multiband operation.

REFERENCES

[1] A. B. Ayed, I. Jaffri, A. M. Darwish, P. Mitran, and S. Boumaiza, "Proof-of-concept of millimeter-wave RF beamforming transmitter architecture employing frequency-multiplier-based up-converters," *IEEE Microw. Wireless Compon. Lett.*, vol. 32, no. 6, pp. 776–779, Jun. 2022.

[2] J.-W. Kim, S.-C. Chae, H.-W. Jo, T.-D. Yeo, and J.-W. Yu, "Wideband circularly polarized phased array antenna system for wide axial ratio scanning," *IEEE Trans. Antennas Propag.*, vol. 70, no. 2, pp. 1523–1528, Feb. 2022.

[3] S. Hong et al., "Applications of self-interference cancellation in 5G and beyond," *IEEE Commun. Mag.*, vol. 52, no. 2, pp. 114–121, Feb. 2014.

[4] A. M. Abbosh, "Compact tunable reflection phase shifters using short section of coupled lines," *IEEE Trans. Microw. Theory Techn.*, vol. 60, no. 8, pp. 2465–2472, Aug. 2012.

[5] W. J. Liu, S. Y. Zheng, Y. M. Pan, Y. X. Li, and Y. L. Long, "A wideband tunable reflection-type phase shifter with wide relative phase shift," *IEEE Trans. Circuits Syst. II, Exp. Briefs*, vol. 64, no. 12, pp. 1442–1446, Dec. 2017.

[6] B. An, G. Chaudhary, and Y. Jeong, "Wideband tunable phase shifter with low in-band phase deviation using coupled line," *IEEE Microw. Wireless Compon. Lett.*, vol. 28, no. 8, pp. 678–680, Aug. 2018.

[7] G. Chaudhary, B. An, and Y. Jeong, "In-band phase deviation minimization method for wideband tunable phase shifter," *Microw. Opt. Technol. Lett.*, vol. 61, no. 2, pp. 537–541, Feb. 2019.

[8] Y. Itoh and H. Takagi, "A dual-band 90-degree SiGe HBT active phase shifter using band-pass and band-stop designs," in *Proc. 47th Eur. Microw. Conf. (EuMC)*, Oct. 2017, pp. 232–235.

[9] Q. Dong, Y. Wu, W. Chen, Y. Yang, and W. Wang, "Single-layer dual-band bandwidth-enhanced filtering phase shifter with two different predetermined phase-shifting values," *IEEE Trans. Circuits Syst. II, Exp. Briefs*, vol. 68, no. 1, pp. 236–240, Jan. 2021.

[10] Y.-P. Lyu, L. Zhu, and C.-H. Cheng, "Dual-band differential phase shifter using phase-slope alignment on coupled resonators," *IEEE Microw. Wireless Compon. Lett.*, vol. 28, no. 12, pp. 1092–1094, Dec. 2018.

[11] Y. Xiong, X. Zeng, and J. Li, "A tunable concurrent dual-band phase shifter MMIC for beam steering applications," *IEEE Trans. Circuits Syst. II, Exp. Briefs*, vol. 67, no. 11, pp. 2412–2416, Nov. 2020.

[12] S. Kim, J. Jeong, G. Chaudhary, and Y. Jeong, "A reflection-type dual-band phase shifter with an independently tunable phase," *Appl. Sci.*, vol. 12, no. 1, pp. 492–504, Jan. 2022.